

COUNTERMEASURE TO SUPPRESS THE FILLING PATTERN DEPENDENCE OF THE BPM ELECTRONICS OF SPring-8 STORAGE RING

Shigeki Sasaki, Takahiro Fujita, JASRI/SPring-8, Sayo-cho, Sayo-gun, Hyogo-ken 679-5198, Japan

Abstract

The signal processing electronics of the SPring-8 Storage Ring Beam Position Monitors (BPM) were replaced during the summer shutdown of 2006, and put into operation. However, a large filling pattern dependence was observed. The cause was attributed to the nonlinear response of the diodes to large pulse signals. The diodes were attached in front of the RF switches for protection from the electrostatic discharge damages on the switch IC. We took a countermeasure for the filling pattern dependence by reducing the pulse height with a band pass filter (BPF) in front of each channel. The BPF were attached and put into the operation from November 2008. The effect of the BPF was evaluated using the beam with changing the filling patterns and repeating the position measurements. The differences of the measured position data across the filling pattern change were found to be within $10 \mu\text{m}$, which was the same amount of the orbit drift during the filling pattern change.

INTRODUCTION

The signal processing electronics of the SPring-8 Storage Ring were renewed in order to improve the performance; better position resolution and shorter measurement time. The obtained resolution was found to be better than $0.1 \mu\text{m}$, and the measurement time became as fast as 3 s from about 20 s for older electronics [1][2]. However, a large filling pattern dependence emerged as large as more than $100 \mu\text{m}$. The current per bunch varies more than two order of magnitude depending on the filling pattern of the Storage Ring. This large difference of the current per bunch result in the same amount of the difference of the signal strength on the pickup electrodes of the BPM. With the large signal strength there were non-linear response of the diodes placed in front of the CMOS radio frequency (RF) switches to protect from the electrostatic discharges.

BPM ELECTRONICS

Figure 1 shows the block diagram of the signal processing electronics. One set of the circuits has 4 line of the signal processing path [3]. Each line covers 3 BPM, i.e. 12 electrodes, since one BPM consists of 4 electrodes. The signals from 12 electrodes are switched sequentially by the multiplexer composed of CMOS RF switch ICs after passing the low-pass filters. The selected signal out of 12 put into the surface acoustic wave BPF (SAW-BPF) and the RF amplifier. The bandwidth of the SAW-BPF is as narrow

as 300 kHz to avoid the non-linearity of the RF amplifier, caused by the revolution frequency harmonics around the RF accelerating frequency. The signal is input to the mixer to be down converted to 250-kHz intermediate frequency (IF). The IF signals pass through the IF amplifier to adapt the signal amplitude to the analogue to digital converter (ADC) input range. The ADC samples the IF signal with the rate of 2MSPS and with the 16-bit resolution. The sampled signals are transferred to the digital signal processor (DSP) board [4] through optical cables. The 250-kHz IF component is extracted by digital demodulation inside the DSP. The position are calculated from the IF component amplitude inside the DSP, and sent to the workstations for the accelerator operation through the ethernet connection.

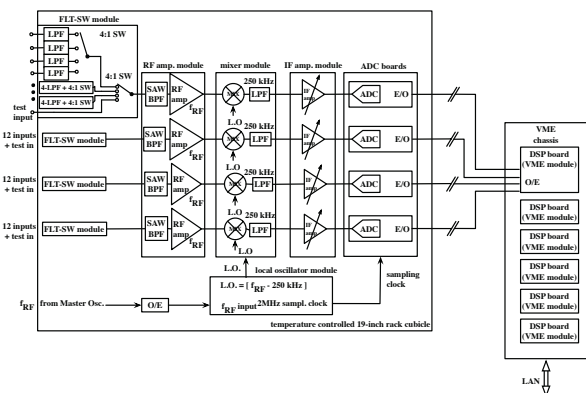


Figure 1: Block diagram of the BPM electronics.

FILTER SWITCH MODULE

The filter switch modules are placed at the front part of the circuits. It contains the low-pass filters, the RF switch and the diodes to protect the switch ICs from excessive voltages. The simplified schematic of the front end part is shown in Figure 2.

The low-pass filter was placed in order to reduce the voltage swing coming from the large current per bunch signals. However, the reduction was not enough for some of the filling patterns. The diodes between the low-pass filter and the multiplexer partially conducted, introduced the non-linearity response on the signal amplitude.

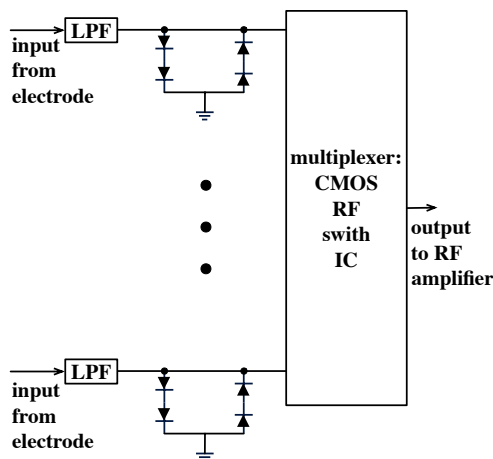


Figure 2: Simplified schematic of the front end part of the BPM signal processing electronics circuits.

BAND PASS FILTER

To solve this problem is to reduce the signal strength further. For that purpose, we attached BPF in front of the LPF. Variation of the characteristics of the BPF within the one set of 4 electrode introduce an artificial error in measured beam position data. The relative difference of 10^{-3} corresponds the $10 \mu\text{m}$ position error, in the case of SPring-8 Storage Ring BPM.

We required the artificial position error to be less than $1 \mu\text{m}$. The requirement corresponded the variation of the attenuation of the pass band to be less than 10^{-4} ($\approx 1\text{m dB}$) within the usage conditions. One of the cause which varies the signal amplitude is the change of the RF accelerating frequency. The RF accelerating frequency of the storage ring change according to the change of the circumference of the ring caused by deformation of the earth by the tidal forces. Another factor of the change of the frequency is the seasonal expansion and shrinkage of the storage ring building. The range of the frequency change is about 1 kHz in a year. This condition requires the pass band flatness to be less than 1 m dB for the range of 1 kHz : $f_0 \pm 0.5 \text{ kHz}$.

The change of the temperature influences the attenuation of the BPF. We specified the temperature coefficient of the centre frequency. The change of the attenuation according to the temperature change is provided by combining the passband flatness of the attenuation and the temperature dependence of the center frequency. The temperature inside the cubicle where the circuits are placed is controlled within ± 0.2 degrees. The pass band attenuation change is obtained roughly by multiplying the temperature coefficient times flatness; $f_0(\text{in kHz}) \times 20 \text{ ppm / deg.} \times 0.2 \text{ deg.} \times 1\text{m dB / kHz} \approx 2 \times 10^{-4}$. The numerical values are quoted from Table 1.

We set the major specification items as in the Table 1. An example of the frequency dependence of the transmission(S_{21}) is shown in Figure 3.

06 Beam Instrumentation and Feedback

T03 Beam Diagnostics and Instrumentation

Table 1: BPF specifications

item	specification
in/out impedance	50Ω
center freq. (f_0)	$508.58 \text{ MHz} \pm 1\text{MHz}$
temp. depend. of f_0	$< 20 \text{ ppm / degree}$
3dB bandwidth	$30\text{MHz}_{\text{max}} \ 20\text{MHz}(\text{typical})$
50dB bandwidth	$250\text{MHz}_{\text{max}} \ 150\text{MHz}(\text{typical})$
passband attenuation	2dB_{max}
flatness	$1\text{m dB} (508.58\text{MHz} \pm 0.5\text{kHz})$
stopband attenuation	$50\text{dB}_{\text{min}} (1\text{MHz}-408.58\text{MHz})$ $40\text{dB}_{\text{min}} (608.58\text{MHz}-1.3\text{GHz})$

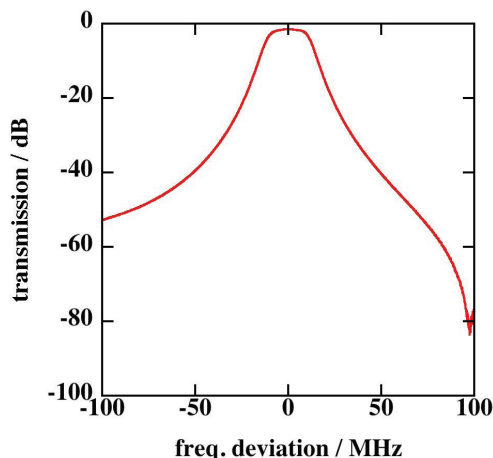


Figure 3: An example of the transmission of the BPF as a function of frequency deviation from the center frequency.

EVALUATION OF THE BPF EFFECT

The first test was done in 2007. Part of the storage ring BPM were attached with BPF and the beam positions were measured for different filling patterns. The result was found to be promising that the differences of the COD values between the different filling pattern were within $10 \mu\text{m}$. We decided to produce the sufficient number of BPF for covering the whole storage ring.

The production finished and all the BPM were attached with BPF in the autumn of 2008 and tested for various filling patterns. We evaluated the effect by the root mean square (rms) values between the two different measurements of the closed orbit distortion (COD), averaged over all the BPM. The rms values were defined as,

$$rms_x(A - B) = \sqrt{\frac{\sum_{i=1}^{N_{BPM}} (x_i^A - x_i^B)^2}{N_{BPM}}} \quad (1)$$

where rms_x is in the horizontal direction, superscripts A and B indicate the two different measurements, i runs through 1 to the number of BPM N_{BPM} , x_i is the measured value in the horizontal direction of i -th BPM. The rms_y , rms value in the vertical direction, is defined in a similar way.

The filling patterns in Table 2 were selected for the evaluation. The explanations of the filling pattern listed in Ta-

Table 2: rms values between the different filling patterns

pattern 1 pattern 2	$\Delta t(\text{min:sec})$	$rms_x/\mu\text{m}$	$rms_y/\mu\text{m}$
multi bunches 203 bunches	24:20	6.8	2.9
203 bunches 1/12 + 10s	19:48	4.2	4.5
1/12 + 10s 1/14 + 12s	21:41	5.9	2.4
1/14 + 12s multi bunches	18:25	4.0	4.3

ble 2 are as followings;

- multi bunches: 12 units, which was composed of 160 sequential buckets filled with some $50\text{-}\mu\text{A}$ current each followed by 43 empty buckets, were equally spaced around the storage ring.
- 203 bunches: equally spaced 203 buckets, i.e. every 12 buckets, were filled with 0.5-mA current each.
- 1/12+10s: Consecutive 203 buckets were filled with electrons; 203 bucket corresponds the 1/12 of the total bucket number of 2436 of the storage ring. The remaining 11/12 part of the ring is filled with equally spaced 10 isolated bunches with 1.5-mA current each, i.e. every 203 buckets were filled with 1.5-mA current. The current of 1/12 part was 85 mA .
- 1/14+12s: Consecutive 174 buckets were filled with electrons; 174 bucket corresponds the 1/14 of the total bucket number of the storage ring. The remaining 13/14 part of the ring is filled with equally spaced 12 isolated bunches with 1.6-mA current each, i.e. every 174 buckets were filled with 1.6-mA current. The current of 1/14 part was 80 mA .

The rms values between different filling patterns in Table2 are all within $10\mu\text{m}$. In order to change the filling pattern, we first discard the stored beam and refill the beam with different filling pattern. It takes about 20 minutes, as shown in Table2 in the column Δt . During these times, the orbit drifts and the rms values increase as large as several μm , even between the same filling patterns. The rms values between the discard and refill of the beam are the same amount of the rms values listed in Table2.

The rms values are plotted in Figure 4 as a function of the elapsed time from the beginning of the measurement. The data jumps between the different filling patterns are the same amount of the jumps between the same filling patterns. The rms values grow almost monotonically because

of the COD drift. All the data points are on the trend of the monotonic growth of the rms values irrespective of the change of the filling pattern.

We concluded that any significant changes were not observed between the filling pattern difference listed in Table 2.

The SPring-8 storage ring has been operated since November 2008 with BPF attached BPM. The continuity of the data between the different filling patterns ensures the stable orbit control of the storage ring across the change of filling patterns.

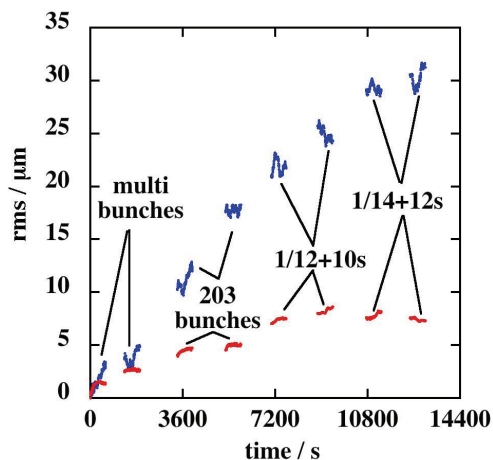


Figure 4: The rms values as a function of the elapsed time from the beginning of the measurement. The blue marks are in horizontal direction rms_x , and the red marks are in vertical direction rms_y .

REFERENCES

- [1] S. Sasaki, T. Fujita, M. Shoji, T. Takashima, gRenewal of BPM Electronics of SPring-8 Storage Ring, Proceedings of DIPAC 2007, Venice, Italy, 20-23 May 2007
- [2] T. Fujita, S. Sasaki, M. Shoji, T. Takashima "Commissioning and Status of New BPM Electronics for COD Measurement at the SPring-8 Storage Ring", Proceedings of PAC07, pp.3997-3999, Albuquerque, New Mexico, USA, 22-25 June 2007.
- [3] S. Sasaki, T. Fujita, M. Shoji, T. Takashima, "Upgrade of BPM Electronics for the SPring-8 Storage Ring" Proceedings of Beam Instrumentation Workshop 2006, Batavia, Illinois 1-4 May 2006, AIP conference proceedings vol.868, pp463-472.
- [4] T. Fukui, T. Masuda, S. Sasaki, T. Takashima, R. Tanaka, gApplications of reconfigurable logic devices for accelerator control, Proc. of ICALEPCS'03, Gyeongju, Korea, 2003